

Characterization of concrete from Roman buildings for public spectacles in *Emerita Augusta* (Mérida, Spain)

María Isabel Mota-López^a, Rafael Fort^b, Mónica Álvarez de Buergo^b, Antonio Pizzo^c, Rubén Maderuelo-Sanz^a, Juan Miguel Meneses-Rodríguez^a, Duygu Ergenç^b

^(a) **Instituto Tecnológico de Rocas Ornamentales y Materiales de Construcción, INTROMAC, Campus Universidad de Extremadura, 10071, Cáceres, Spain.**

^(b) **Instituto de Geociencias (CSIC, UCM), José Antonio Nováis 12, 28040, Madrid, Spain.**

^(c) **Instituto de Arqueología de Mérida (IAM-CSIC). Plaza de España 15, 06800, Mérida, Spain.**

Abstract

The present study focuses on the compositional characterization of Roman concrete from Roman buildings for public spectacles, theatre and amphitheatre, from *Emerita Augusta*, Mérida, Spain. An advanced knowledge of the Roman concrete composition is required to get a reliable restoration and preservation of these ancient monuments. The concrete was studied through mineralogical (petrographic microscope and X ray diffraction) and petrophysical (bulk and real density, open porosity, mercury intrusion porosimetry, compressive strength and ultrasonic pulse velocity) analyses. With this work, it is possible to fill the gap which exists in this field, the characterization of the materials used in the Roman concrete from these two buildings, never previously studied, despite the significance of this archaeological ensemble, declared a World Heritage Site by UNESCO in 1993. The obtained results of the studied samples, allowed us to determine the composition of the concrete and to infer the provenance of the aggregates used in it.

Keywords: Roman concrete; Heritage; Mineralogical analysis; Petrophysical analysis; Provenance.

1. Introduction

The restoration of historical buildings is very important for the history and culture of the cities and their population. The restoration of these buildings, of great importance in architectural heritage, requires an advanced knowledge of the building materials used to build these monuments. Traditional materials such as natural stone (granites, marbles, etc.), bricks, mortars and concretes, were used in the construction of these historical buildings. In general, natural stone and woods were extracted near the cities (Malacrino 2010; Fort et al. 2010; Tucci 2014). Historic mortars and concretes can reveal different compositions and the dependence on the geographical location and the time period of its construction (Kramar et al. 2011; D'Ambrosio et al. 2015; Marra et al. 2015). In restoration works, design and application of a repair mortar that will closely match with the existing historic materials and that can replace the original Roman concrete, require an extensive and an elaborated work to be carried out within a complete framework.

Although lime based mortars have got an increasing interest in the monuments conservation (Pacheco-Torgal et al. 2012), they show a slow hardening binder that reach times, in some cases, more than 1 year. These can be solved by the use of formulations containing pozzolanic additions. The use of pozzolanic materials in construction as hydraulic binder dates back from thousands years ago (Roy and Langton 1989; Malinowsky 1991). The Roman mortars were made of artificial (calcined clays or crushed ceramic material) or natural pozzolans (ashes) mixed with lime binder. Lime was the main binder used until the use of Portland cement in the 19th century (Varas et al. 2005). The appearance of Portland cement-based mortars came to dethrone air lime mortars due to its higher mechanical strength and a low setting time, allowing for work completion in relatively short period (Pacheco-Torgal et al. 2012). Some authors found that some lime-cement mortars are more appropriate than hydraulic lime mortars (Mosquera et al. 2002; Arandigoyen and Alvarez 2006, 2007), ensuring a minimum mechanical strength at early ages (Elpida-Chrissy et al. 2008) or allowing more deformation in the masonries (Cizer et al. 2008). Although it is true that, in some inadequate restoration interventions, the use of Portland cement-based mortars can cause more damage than benefit through negative interactions between the cement and the original materials (bricks, stones or binders) (Colleparidi 1990), due to less permeability and a high modulus of elasticity (Gleize et al. 2009), or the appearance of alkali carbonate and bicarbonate salts and the damage mechanism of salt crystallization, related to the pressure of salts in the pore radius (Scherer 1999; Flatt 2002), if Portland cement is used in a small amount this will remain a minor problem and it is not supported by scientific evidence (Pacheco-Torgal et al. 2012). Therefore, previously to any intervention in historical buildings, it is necessary a historic-scientific study of the original mortar with the object to obtain a restoration mortar; lime-pozzolan; lime-cement mortar or Commercial pre-pack mortars for conservation purposes, that shows a similar mechanical behaviour and physical-chemical characteristics trying to use the current materials compatible with old building materials (Lourenço 2006).

Historical concretes are complex systems that contain aerial or hydraulic binders or a blend of them, with aggregates, not always crystallines, and other elements that interact with the binder (Moropoulou et al. 2000). The use of different techniques for micro-structural characterization of materials, like optical microscopy, X-ray diffraction or petrophysical analysis, allows the determination of the composition and some properties of these concretes. However, each technique has its owns limits and, in many cases, several characterization techniques must be used to get coherent and reliable results (Paama et al. 1998).

The purpose of this paper is to characterize the ancient concrete from the Roman theatre and amphitheatre from *Emerita Augusta*, Mérida, Spain, one of the most important cities in *Hispania*, founded by the Romans in the first half of the first century B.A., and to determine the provenance of its aggregates. This study will also be very useful in case of any Roman concrete replacement should be performed in the future.

2. Roman buildings for public spectacles in *Emerita Augusta*: brief historical overview

Emerita Augusta, currently Mérida (Extremadura, Spain), is the symbol of the process of Romanization in a land that had hitherto not been influenced by the urban phenomenon. It contains the substantial remains of a number of important elements of Roman town design, considered to be one of the finest surviving examples of its type and declared a World Heritage Site by UNESCO in 1993 (<http://whc.unesco.org/es/list/664>). It was founded by Emperor *Augustus* in 25th B.A., in order to make a retirement place for war veterans from *V Alaudae* and *X Gemina* legions that fought in Cantabrian wars and became the capital of *Lusitania* province, as one of the most important cities in the Roman Empire (Ortiz et al. 2014).

The main buildings used for public events in the ancient Roman Empire were the theatre, the amphitheatre and the circus. Unfortunately, afterwards the structures of this latter were almost lost, only keeping its entire plant with a rectangular path ending in a semicircle (Mateos and Pizzo 2011). The theatre, considered among the most important theatres from the Roman world by its conservation state, was built in 16th B.C (Fig. 1). It has a semicircular floor plant with 86.63 m in diameter and a *pulpitum* with 59.90 x 7.28 m in a rectangular floor plant (Durán Cabello 2004). The seats are arranged in tiers, leaning on St Albin hill, having a capacity of approximately 5,500 spectators (Mateos 2001). The masonry walls are composed of granite ashlars that enclose the *opus caementicium* (Fig. 2-a), a mixture of water, rocks and bricks fragments having different sizes and shapes, as aggregates, and slaked lime as binder. The amphitheatre was built in 8th B.C. close to the theatre and was modified until first century. It was designed at the same time than the theatre, far from the city walls, that were corrected when both buildings were enlarged due to the necessity of its use. Its design consists of a grandstand, 126.30 m long and 102.65 m wide, with *ima*, *media* and *summa cavea* and a central *arena* (64.50 m long and 41.15 m wide) (Bendala Galán and Durán Cabello 1995) (Fig. 1). The masonry walls are composed of quartzite blocks, irregular shaped, joined by mortar, and granite ashlars that enclose a concrete core or nucleus, composed by various types of coarse aggregate, bound together by relative well-preserved mortar (Fig. 2-b). The stands had a capacity of approximately 15.000 spectators and an available *scalae*, stairs and hallways that connected the different parts -*cunei*, wedge-shaped seating sections in the cavea (Pizzo 2007; Mateos and Pizzo 2011). There were 26 numbered doors to let spectators in and out, called *vomitorium*.



Fig. 1. Aerial overview of the theatre and amphitheatre of *Emerita Augusta* by courtesy of the Consortium “Monumental Historical-Artistic and Archaeological City of Mérida”.



Fig. 2. External wall from the theatre (left) and amphitheatre (right).

3. Geological setting

Extremadura is geologically located in the Iberian Massif, being part of the Central Iberian Zone, in the north of the region, and the Ossa-Morena zone, in the south of it. The Central Iberian Zone is characterized by the abundance of clastic metasedimentary rocks and greywackes, sandstones, shales, conglomerates, quartzites and less in carbonate materials such as limestone and dolostone. Also it is highlighted with the Hercynian granitic intrusions. The rocks from the Ossa-Morena zone are metamorphic and igneous, both intrusive and volcanic.

Merida batholith is located in an area framed by a line between Mirandilla (12 km NE from Merida), Proserpina (5 km to the north of Merida) and Esparragalejo (8 km NW from Merida) and is part of a regional magmatic alignment with the batholiths of Alburquerque and Los Pedroches. Granites are the most common rocks in the area of Merida, constituting more than 50% of the outcrops (Gonzalo 1987). Granites appear in three main elongated plutons through the NNW–ESE trending. These plutons are Sierra Bermeja pluton, located at the north of the above Sierra; Proserpina pluton, located at the W-NW from Merida city; and Valdetorres pluton, located at the West from Guareña (Gonzalo 1987). Sierra Bermeja pluton consists of two facies: one is the central facies which is an equigranular medium grained two-mica monzogranite with cordierite, the other is biotitic porphyritic granite ranging in composition between granodiorites to monzogranites that have thickness between 0.5 to 1.1 km. Proserpina pluton shows four facies, biotitic porphyritic granite; two-mica granite with fine grain size, aplitic granite and monzogranite with cordierite. Valdetorres pluton consists of two facies, monzogranite with cordierite with medium grain size and very homogeneous and biotitic porphyritic granite surrounding the latter facies (Fig. 3).

These granites were intruded during Devonian-Permian times into a pre-Cambrian basement made up by black slates and schists, quartzites, amphibolites and diorites rocks that belong to a previous plutonism, and carbonated rocks from Cambrian. Carbonated outcrops are located 5 km to the north of Merida, scattered over the Proserpina pluton, made up by limestones and dolostones which are covered by Guadiana river depression sediments in some zones. These Lower Cambrian outcrops belong to the Alconera Formation (Liñán and Perejón 1981). This formation appear over granites which sometimes cross them, and the amphibolitic serie and diorites or calco-silicate schists, formed by massive limestones alternated marls and dolostones, going to top levels to dolostones and dolomitic marbles having pink and gray shades which in contact with the limestone layers, show levels and chert nodules. These limestones and dolostones show a strong recrystallization due to the contact metamorphism of the Merida's batholiths. This formation is well represented by the Carija Slope and North Araya slope, having 100 m (Fernández-Caliani et al. 1996).

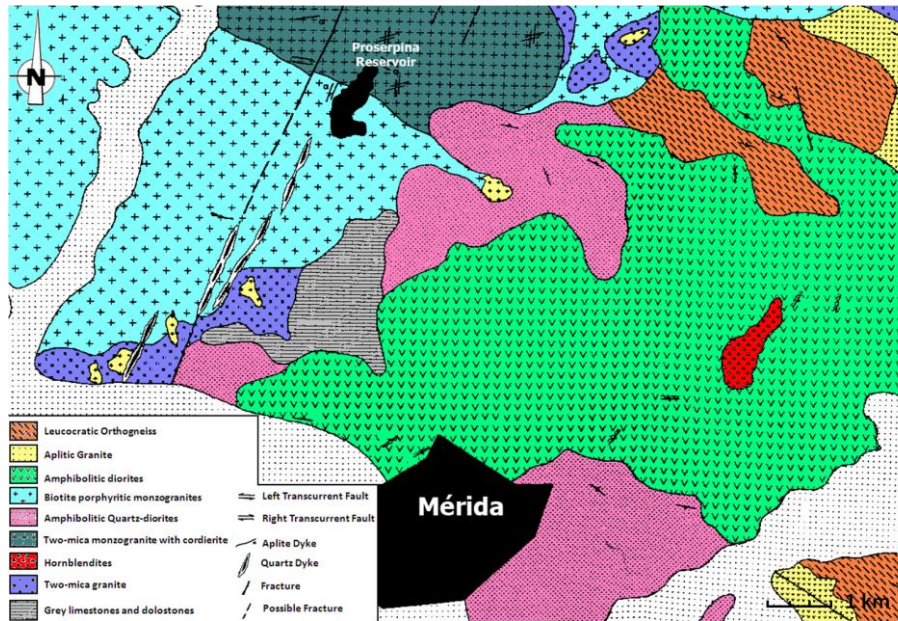


Fig. 3. Geological scheme of the Mérida area, modified from Gonzalo (1987).

The city of Mérida is crossed by Guadiana river to the Southwest, and show terraces and flood plain having rounded boulder quartzites and sandy matrix which can be cemented in terrace levels by carbonates, limes and fine sand show up in top levels. To the North the city is crossed by Albarregas river that shows rounded quartzites and sand.

This geographic zone has suffered different tectonic phases due to the great isoclinal folds, convergent to the Northeast in Precambrian materials and the Cambrian carbonatic formation having concentric folds with SO direction. After the Merida's batholith intrusion, which created the low level metamorphism over this materials, and the easing phases with fault systems, mainly in the direction N 125°-135° E, N 65°- 75° E and the leucogranito dikes and quartz veins, diabases, aplites and porphyries (MAGNA 2003).

4. Materials and methods

Due to the historical classification of these buildings, which belong to the Archaeological Ensemble of Mérida, listed as World Heritage Site in Spain, the sampling of the concrete was very restricted even with legal authorization from the competent institution in charge of the structures. Twelve concrete samples were taken from the amphitheatre and four samples from the theatre, being these samples representative enough for the whole building (Table 1 and Fig. 4). The location of the samples is shown in Fig. 4.

The samples were cut from a concrete core (5 cm diameter) extracted from inside the masonry walls, trying to obtain an undamaged material (Fig. 5). A sufficient quantity of sample was taken to allow the development of the entire set of planned analyses in all cases. The external and more decayed part of the samples was removed and discarded in order to ensure the collection of non-altered material (Álvarez et al. 1999).

Thin sections were prepared, previously consolidating the samples with epoxy resins to avoid disintegration in the process, and examined using a polarizing optical microscopy (Leica Leitz Laborlux 12 POL S) and images were recorded digitally (JVC Digital Colour Camera TK-C1480E). Thin sections were stained with red alizarin for the differentiation of carbonates (red stained, calcite; non-stained, dolomite).









Sample	Location	Picture
Theatre		
T_HR-1	Right area of vomitorium N° 11	
T_HR-2	Right area of vomitorium N° 9	
T_HR-3	Left area of vomitorium N° 7	
T_HR-4	Right area of vomitorium N° 7	
Amphitheatre		
A_HR-1	Right area of vomitorium N° 9	
A_HR-2	Left area of vomitorium N° 9	
A_HR-3	Right area of vomitorium N° 9	
A_HR-4	Right area of vomitorium N° 9	
A_HR-5	Left area of vomitorium N° 8	
A_HR-6	Left area of vomitorium N° 8	
A_HR-7	Summa cavea between vomitoriums N° 4 and N° 5	
A_HR-8	Summa cavea between vomitoriums N° 4 and N° 5	
A_HR-9	Summa cavea between vomitoriums 16 and 17	
A_HR-10	Summa cavea between vomitoriums 16 and 17	
A_HR-11	Left area of vomitorium N° 15	
A_HR-12	Left area of vomitorium N° 15	

Table 1. Location and description of the sample mortars from the amphitheatre and theatre.

Mineralogical characterization was performed through X-ray diffraction (XRD) with a Philips X'Pert Pro diffractometer equipped with a goniometer PW 3050 with CuK α radiation, operating at 45 kV and 40 mA. The powder sample was mounted on a quartz support to minimize background. Samples were dried at 55 °C, crushed and sieved prior to XRD analysis.

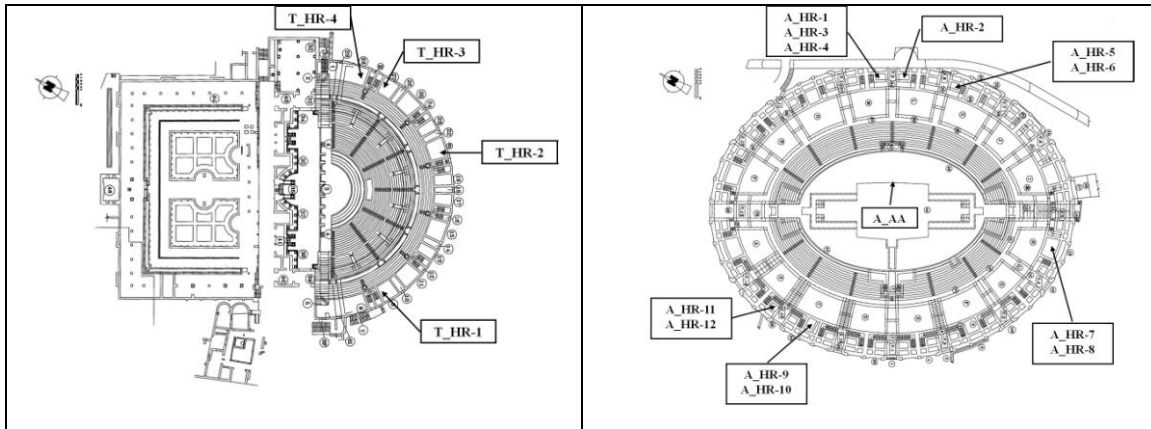


Fig. 4. Locations of the sampling of the studied concretes in theatre (left) and amphitheatre (right). Plan from Duran Cabello (2004).

The bulk and real densities, the open porosity (porosity accessible to water), capillary coefficient and the compressive strength of the concrete were determined according UNE EN 1936:2007 and UNE EN 1926:2007 standards, respectively. The compressive strength was determined using a test machine from Sistemas de Ensayo, S.L., type CMED-AR-200/SDC. The loading force was measured by a loading cell with capacity 200 N, operating under load control. The binder/aggregate ratio was determined by the dissolution of the mortar samples through hot hydrochloric acid attack, as described by Álvarez et al. (1999).

Ultrasonic equipment (PUNDIT, C.N.S. Electronics, 54-MHz transducer) was used to measure the ultrasound pulse velocity through direct measurements on samples in the laboratory. In order to measure the pulse velocity with a high degree of accuracy, a good acoustic coupling between the transducer face and the samples surface was achieved by using a suitable couplant. Mercury intrusion porosimetry was applied to the study of pore structure of the historic Roman concrete, using an AutoPore IV 9500 (Micromeritics Instrument Corporation), with a pressure ranging from 0.00345 to 230 MPa, allowing the study of pore sizes in the range 600–0.0035 μm . The contact angle of the mercury was assumed to be 117° in concrete (Laskar et al. 1997). Surface tension and equilibrium time considered was 0.485 Nm^{-1} and 20 s, respectively. For each sample, 2.5 g of each specimen were analyzed.

Thermogravimetric Analysis and Differential Scanning Calorimetry (TG-DSC) was used to classify mortars as typical lime mortars, hydraulic mortars or pozzolanic mortars. It was performed with a TA Instruments SDT-Q600, DSC Q-200 and General V4.1C DuPont 2000 thermogravimetric analyzer, respectively, in a nitrogen (N_2) atmosphere at a heating rate of 10 °C/min within the temperature range $T_{\text{amb}} - 1000$ °C.

Scanning electron microscopy employed a Jeol JSM-820 microscope equipped with an energy dispersive X-ray analyser (EDX), using an accelerating voltage of 20 kV. Samples were coated with gold film before SEM-EDS analyses.



Fig. 5. Photographs of the concrete samples T_HR-1 (a), T_HR-2 (b), A_HR-6 (c) and A_HR-11 (d).

5. Results and discussion

5.1. Macroscopic description

The concrete samples from both monuments were characterized by aggregates having sizes up to 10 cm (Fig. 5) and a whitish binder, observing, in the case of the theatre, fragments of gray granite (2 cm), quartzite (4 cm), feldspars and ceramic, besides the presence of pores having different sizes. The aggregates show coarse grain sizes, larger than 2 cm. In the case of the amphitheatre, the mortar samples, according to macroscopic observation of the type of aggregate used, could be separated into two categories, those that present fragments of green schists (A_HR-1, A_HR-3, A_HR-5, A_HR-6, A_HR-7, A_HR-10, A_HR-11), and those that present fragments of metamorphic rocks (A_HR-2, A_HR-4, A_HR-8, A_HR-12). The aggregates in these samples showed a coarse grain size, ranging from 2 cm to 7 cm. These aggregates, minerals and rock fragments, showed sub-angular to rounded shape.

5.2. Petrographic analysis

The petrographic analyses revealed the presence of calcite (binder areas were red stained), having a micrite size, resulting from the carbonation of the lime used as binder (Velosa et al. 2007). This fine-grain size is the responsible for the cohesive petrofabric of the lime binders studied, displaying a perfect aggregate bond and scarce fissures that suggest a high reactivity, water retention capacity and low shrinkage of the lime (Pavía and Caro 2008), fissures that usually are present in ancient mortars or concretes having low quality (Malinowski 1979). Besides, it could be shown the presence of numerous tiny pores (0.06 mm to 1.15 mm), having inter-granular type, in certain zones. Micrographs of T_HR-3, T_HR-4, A_HR-4, A_HR-6, A_HR-7 and A_HR-12 samples are shown in Fig. 6.

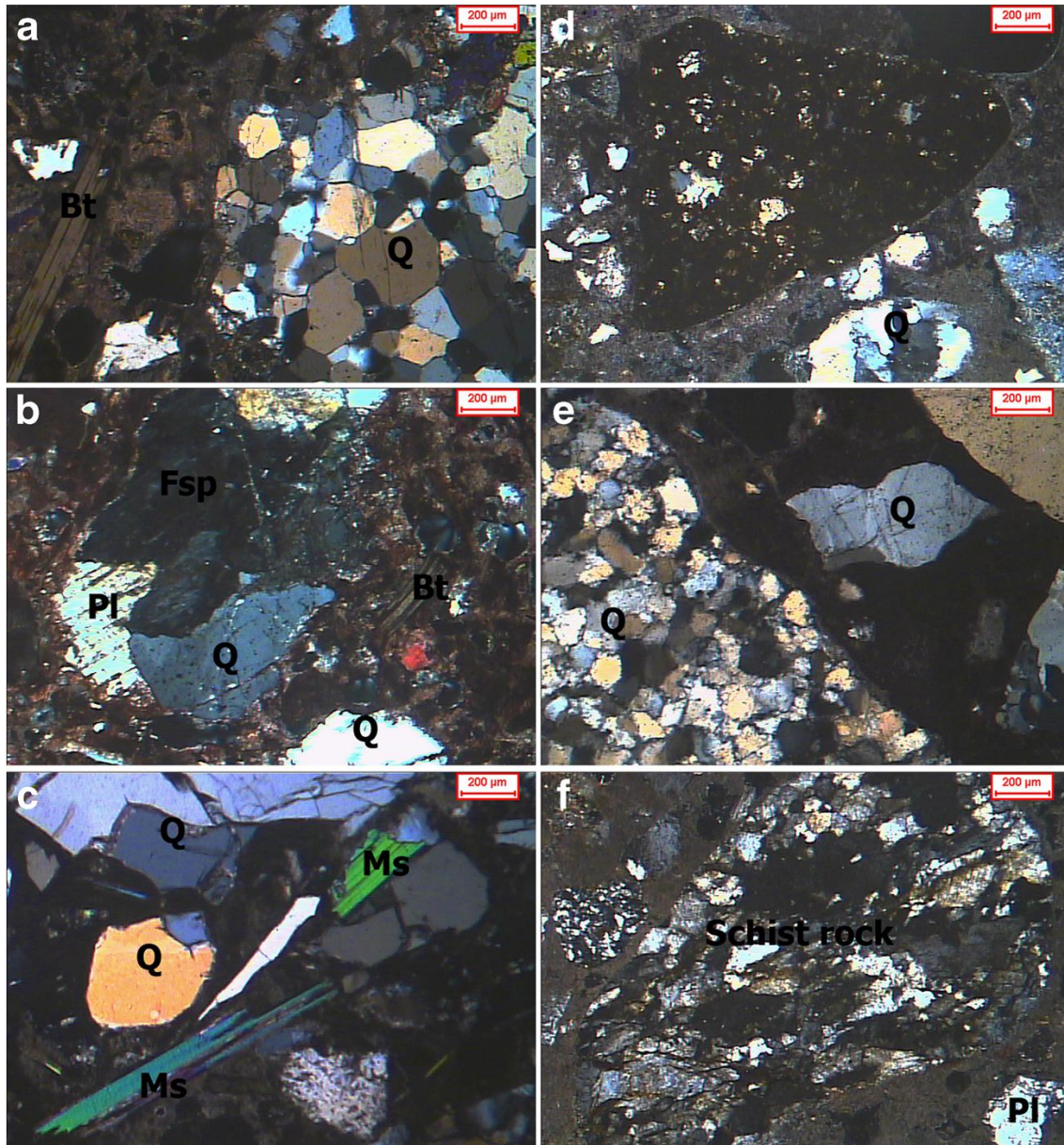


Fig. 6. Thin-section images of the mortar samples in crossed polars. (a) Sample T_HR-3. Biotite grains and a fragment of quartzitic rock made of a quartz grains mosaic, in a carbonated matrix and the presence of pores. (b) Sample T_HR-4. Angular quartz grains, potassium feldspar, plagioclase and biotite in a carbonated matrix. (c) Sample A_HR-12. Rounded clast of quartz (left) and muscovite grains floating in a carbonated matrix. Some pores and fractures are present in the sample. (d) Sample A_HR-4. Polycrystalline quartz and angular ceramic fragment floating on a fine-grained cohesive lime binder. (e) Sample A_HR-6. Angular

quartz grain and a fragment of quartzitic rock, made up of a mosaic of quartz grains, in a carbonated matrix. (f) Sample A_HR-7. Fragment of schist rock and plagioclase floating in a carbonated matrix.

The nature of the aggregates was variable, being composed of minerals and rock fragments. Mineral aggregates were composed by medium to coarse-grained monocrystalline and polycrystalline quartz, potassium feldspar, plagioclase and biotite; fine to coarse-grained muscovite and coarse-grained microcline, with roundness of grains varying from sub-angular to sub-rounded and low sphericity. Rock fragments were mainly quartzite, which is indicative that these aggregates come from the same zone (Kramar et al. 2011), close to Albarregas river or Guadiana river, limestone, granitic rocks, schists (samples A_HR-5, A_HR-7 and A_HR-9, where it could be seen the presence of tremolite-actinolite, porphyry, diorites, calcareous rocks and ceramic fragments. The presence of these aggregates was indicative of the re-use of waste materials for the construction of this monument (Zamba et al. 2007). It was very interesting that the presence of schistose rocks in the aggregates would account for the use of the bed rock that outcrops in the middle of the *arena* (Fig. 7), which was mineralogically classified as tremolite-actinolite schist. These clasts, rock fragments, had medium-low sphericity and angular to sub-angular roundness.

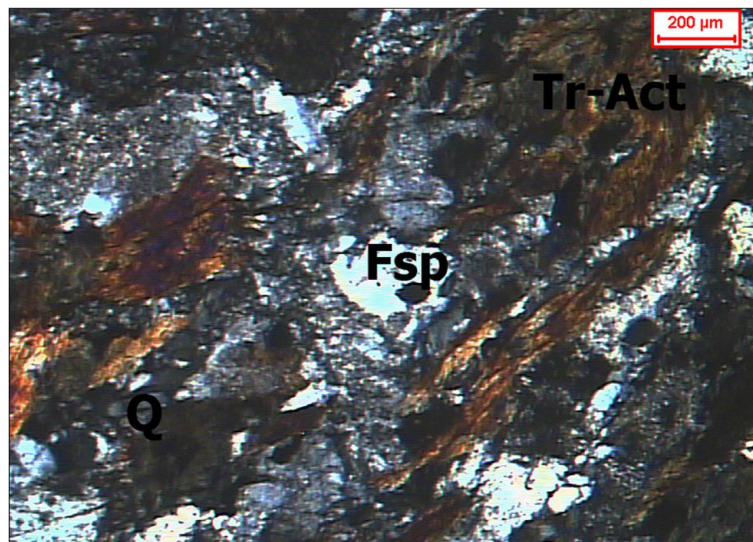


Fig. 7. Thin-section observation of the sample from the *arena* outcrop in cross polarized light. Sample A_AA. Nematogranoblastic rock, with quartz grains, potassium feldspar and tremolite.

5.3. Mineralogical analysis (XRD)

The mineralogical components of concrete characterized by XRD revealed us that the main components of the mortar were quartz and calcite (Fig. 8). Other constituents were potassium feldspar, plagioclase, biotite, ilmenite, chlorite and tremolite-actinolite. These results were consistent with that of the petrographic observations. Samples A_HR-5 and A_HR-7 showed the presence of tremolite-actinolite as aggregates, which was indicative of the provenance of this aggregate, coming from the outcrop in the *arena*. These concretes presented calcareous binder having mainly siliceous aggregates, feldspars and mica minerals. The presence of calcite could be interpreted as the binder, as a result of the lime carbonation (Pavía and Caro 2008).

5.4. Petrophysical analysis

The results obtained for bulk density (Table 2) showed that the values are slightly higher to those found by other authors in similar materials (Drdácky et al. 2013) and possibly due to the presence of larger aggregates and the low porosity of these aggregates (granites, quartzite and schistose rocks). The low porosity could be a result of the addition of ceramic fragments (Moropoulou et al. 1995, 1998a, 1998b). The differences between real and bulk densities were due to the high values of porosity of the samples (Table 2).

Sample	Open porosity (%)	Bulk density (g cm ⁻³)	Real density (g cm ⁻³)	Capillary coefficient (g m ⁻² s ^{-1/2})	Hg porosity (%)	Compressive strength (MPa)	Ultrasound velocity (m s ⁻¹)
T_HR-1	29.5	1.810	2.489	5.14	32.9	25.2	1492
T_HR-2	17.0	2.140	2.518	4.50	20.6	36.5	1758
T_HR-3	12.5	2.312	2.567	4.06	20.5	38.5	1654
T_HR-4	21.4	2.210	2.440	3.95	23.3	35.4	1635
A_HR-1	5.9	2.010	2.497	3.93	20.6	32.6	2066
A_HR-3	2.4	2.168	2.404	3.21	-	50.1	2147
A_HR-4	8.6	1.970	2.433	2.96	-	46.5	2125
A_HR-5	15.5	2.260	2.419	3.52	27.2	38.2	2014
A_HR-6	17.4	2.260	2.532	5.26	25.7	41.2	1998
A_HR-7	28.7	1.850	2.563	7.99	30.8	27.3	1767
A_HR-8	18.7	1.940	2.447	5.04	-	39.5	1954
A_HR-9	20.4	2.140	2.527	4.17	23.2	25.0	1552
A_HR-10	22.4	2.210	2.535	4.22	25.2	37.5	1887
A_HR-11	18.0	2.100	2.416	1.93	36.3	47.6	2168
A_HR-12	16.0	2.170	2.496	5.96	29.8	48.4	1660

Table 2. Real and bulk densities, open porosity, capillary coefficient, Hg porosity, compressive strength and ultrasound velocity of the concrete from the samples from the amphitheatre and theatre.

Samples T_HR-1, A_HR-7 and A_HR-10 showed the highest open porosity, with an average value of 26.9 ± 3.9 %, while samples A_HR-1, A_HR-3 and A_HR-4, showed a relatively low porosity, having an average value of 5.6 ± 3.1 %, due to the presence of aggregates with different sizes, that is to say, being larger in the former than the latter. These values were similar to others found by another authors (Moropoulou et al. 2005; Sánchez-Moral et al. 2004; Hughes et al. 2007; Theodoridou et al. 2013).

The values of capillary coefficient were relatively high. This was due to the values of porosity (Table 2) and the pore size distribution where pores having sizes greater than $0.1 \mu\text{m}$ were responsible for the capillary movement (Winkler 1997). Samples from the theatre showed similar values, having the sample T_HR-1 a slightly greater value due to the presence of fine pores with the threshold diameter below $0.1 \mu\text{m}$ (Fig. 9-a). For the amphitheatre, sample A_HR-11 had the lowest value of capillary coefficient due to the major distribution of pore sizes in the range $0.003 \mu\text{m}$ to $0.020 \mu\text{m}$. For the sample A_HR-7, a distribution of pores between $0.1 \mu\text{m}$ and $0.5 \mu\text{m}$ was the responsible of the greater value of the capillary coefficient for the samples of the theatre. In the rest of the samples, there was a coexistence of fine pores with the threshold diameter below $0.1 \mu\text{m}$ and of larger pores with diameters between 0.8 - $100.0 \mu\text{m}$ (Fig. 9-b).

The compressive strength values of the samples were relatively high, values that range between 25.0 MPa and 50.1 MPa, compared to other ancient concretes (Drdácky et al. 2013; Giavarini et al. 2006). This was due to the pozzolanic reaction of the ceramic particles with lime and the presence of siliceous aggregates having larger sizes. The values of the compressive strength were agree with those of porosity, therefore, samples having low values of porosity, have higher values of compressive strength (Chen et al. 2013). Samples A_HR-3 and A_HR-4, having low values of compressive strength and lower values of porosity could indicate that their state of conservation is better than the other samples. The results of ultrasound velocity showed that the values obtained in the amphitheatre are higher than the theatre so this could be due to the nature or the size of the aggregates, the relationship between the binder and the aggregates or due to the ultrasound velocity which is directly related to the presence of voids, holes, cracks or fractures in the concrete, causing the decreasing of the velocity of the ultrasound waves.

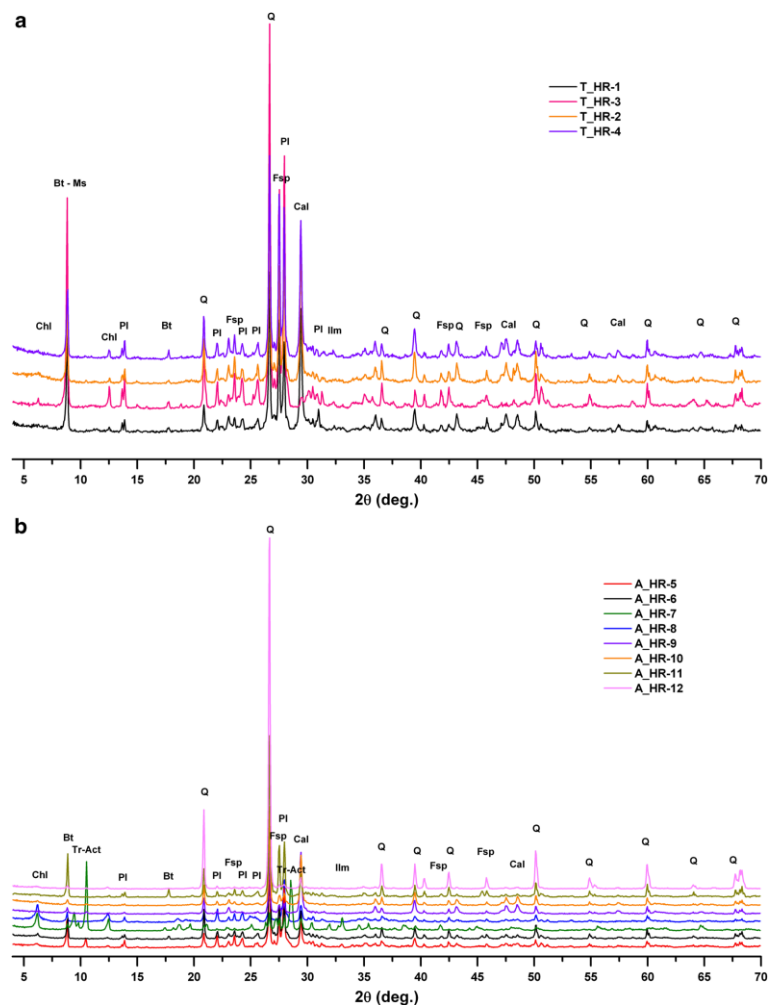


Fig. 8. XRD patterns from theatre (a) and amphitheatre (b) mortar. (*Bt*: biotite, *Cal*: calcite, *Chl*: chlorite, *Fsp*: potassium feldspar, *Ilm*: ilmenite, *Ms*: muscovite, *Pl*: plagioclase, *Q*: quartz, *Tr-Act*: tremolite-actinolite).

Usually, the values of porosity from the mortar that belongs to the Roman concrete, obtained through mercury intrusion porosimetry, are very variables (Pavía and Bolton 2000). Table 2 shows that, in the studied samples in this work, this value was ranging between 20.6 % and 36.3 %. The porosity values coincided with those found in other ancient lime mortar from Roman time (Moropoulou et al. 2005; Sánchez-Moral et al. 2004; Hughes et al. 2004; Theodoridou et al. 2013) or other historic times (Farci et al. 2005; Sandrolini and Franzoni 2010; Borges et al. 2014).

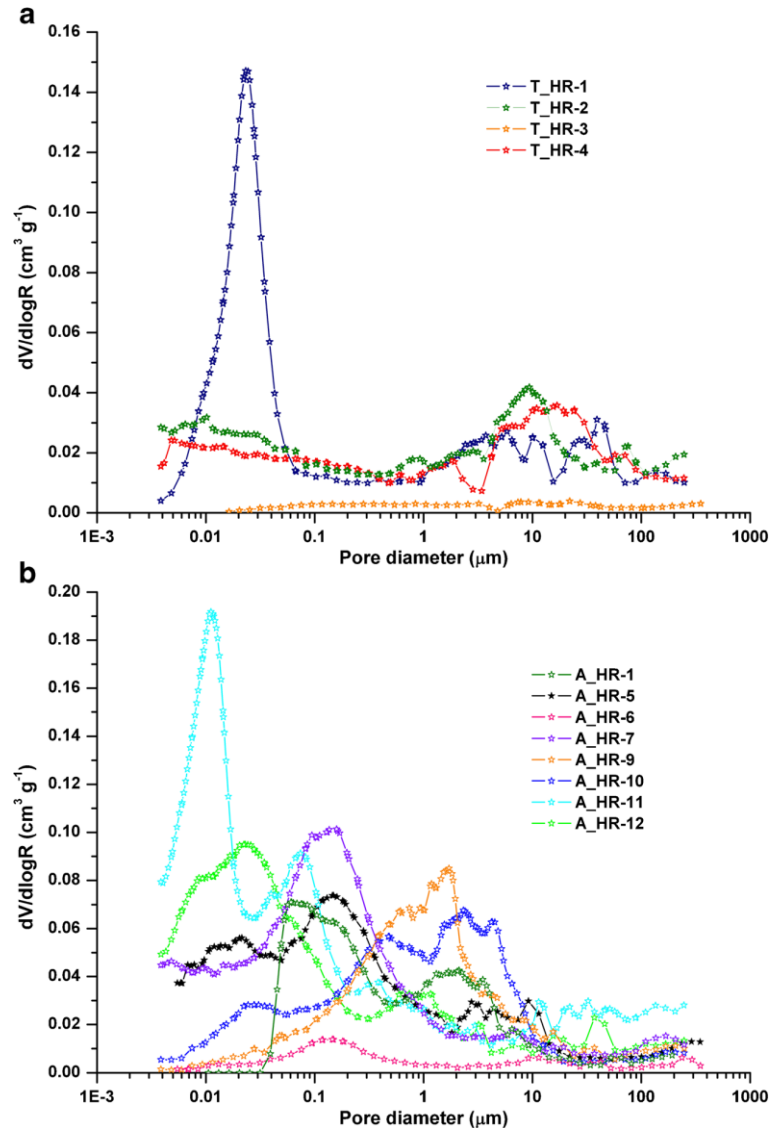


Fig. 9. Differential volume of intruded mercury vs pore diameter for the samples of the mortar from the theatre (a) and the amphitheatre (b).

To determine the binder/aggregate ratio of the mortars, the method of hot HCl attack (Álvarez et al. 1999) allowed the classification of the mortars into four groups: 1:1 (A_HR-10), 1:2 (T_HR-1, T_HR-2, T_HR-3 and A_HR-1) and 1:3 (A_HR-2, A_HR-6, A_HR-7, A_HR-11, A_HR-12, T_HR-4 and A_HR-4). In the case of the samples A_HR-3 and A_HR-8, the binder/aggregate ratio showed abnormal values, 1:6 and 1:9, respectively, due to the presence in the samples of large aggregates, having sizes higher than 7 cm.

Fig. 9 shows the differential mercury intrusion curves, i.e. incremental pore volume intruded as a function of pore diameter for the mortar samples, where it could be observed some differences between samples from the theatre and the amphitheatre. The pore size distribution was more homogeneous in case of the theatre, with the exception of the sample T_HR-1, in which the aggregate sizes were lower than the other samples from the theatre. In the amphitheatre, the pore size distribution was not homogeneous. The aggregate sizes in these samples were more variable. Due to the homogeneity found in the pore size distribution for the samples coming from the theatre, petrophysical properties for this monument were less variable than in the amphitheatre, where it could found open porosity values ranging between 2.4 % and 28.7 %, or compressive strength values ranging between 25.0 MPa and 50.1 MPa. The shape of the

differential mercury intrusion curves, where there were a wide range of pore sizes, was due to the larger pores that could be related to micro-cracking or contact between aggregates, and the smaller pores could be related to the binder. In the theatre, for the sample T_HR-1 only one peak was observed but one could hardly speak about a uni-modal pore size distribution as the peak was slightly broad and resulting of the superposition of a range of pore sizes between 0.005 μm and more than 0.080 μm , having medium pore size of 0.019 μm . For the samples A_HR-5, A_HR-7 and A_HR-12, in the amphitheatre, happened something similar than for the sample T_HR-1. In these samples, the peaks were very broad as a result of the superposition of a range of pore sizes between 0.030 – 1.000 μm , 0.010 – 1.000 μm , and 0.005 - 0.200 μm , respectively, having medium pore size, between 0.022 μm and 0.076 μm , due to the addition of ceramic particles with low size (around 600 μm) (Kramar et al. 2011). Sample A_HR-11, was different from the rest of samples, because exhibited a bimodal distribution of pore sizes, having two well distinguished peaks, 0.010 μm and 0.080 μm . The presence of the peak indicates a one-step intrusion of mercury into a capillary network connected to the specimen surface. It showed a great distribution of pore sizes that could be attributed to the different binder/aggregate ratio of the mortars, degree of compaction or the age of the mortars (Theodoridou et al. 2013). The values of open porosity were lower than Hg porosity. This was due to the presence of an important contribution of the micro-porosity, more intense in the case of the amphitheatre.

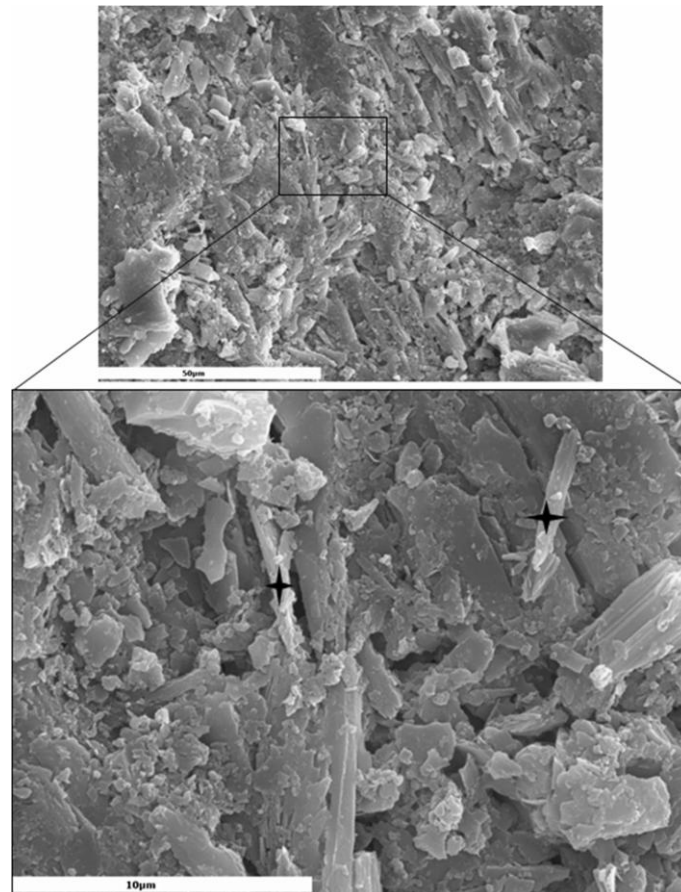


Fig. 10. SEM micrographs of T-HR-3 sample showing the needle shape calcium silicate aluminium hydrate (CSAH) crystals in the border of the binder and ceramic fragment (EDS analysis on the points indicated in the picture with black star show the presence of Ca, Si, Al and Fe).

The presence of ceramic fragments in the Roman concrete, suppose the addition of pozzolanic effect in this material. In the absence of natural pozzolanic material such as that available in volcanic regions, Romans employed ceramic particles and dust to fulfil the same role (Pavía and Caro 2008; Theodoridou et al. 2013; Moropoulou et al. 1995; Baronio and Binda 1986; Elsen 2006; Franquelo et al. 2008; Robador

et al. 2010). The pozzolanic effect is attributed to the adhesion reaction that happens in the interface ceramic fragments and the matrix, in which calcium silicate is formed (Fig. 10). SEM-EDS give additional information about the microstructure of the binder, aggregate and reactions between them. In all mortars quartz aggregates and brick fragments were detected as embedded in the lumpy appearance calcitic lime binder. Needle like CSAH crystals are observed inside the cracks and pores of the ceramic fragments and in the boundary between aggregate and binder. Lime can seep inside de ceramic fragments, and can reduce the pore size, increasing real density, achieving a great compression strength in the Roman concrete (Moropoulou et al. 2003, 2005). This can explain its acceptable conservation state and stability in the time.

Table 3 shows the results obtained of the thermogravimetric analysis. Moropoulou et al. (2005) and Bakolas et al. (1998), proposed a classification to classify mortars. According to this classification, the weight loss up to 120 °C is due to adsorbed water, characteristic of the presence of hydraulic binders that are hygroscopic. In the range 120–200 °C, the weight loss in the temperature, is attributed to the crystallization water of hydrated salts that may originate from the sulphation of carbonates or the accumulation of salts in the masonry. The weight loss between 200 °C and 600 °C is attributed to the loss of the structurally bound water to hydraulic products, such as calcium silicate hydrates or calcium aluminate hydrates. The weight loss above 600 °C is due to carbon dioxide released during the decomposition of calcium carbonates. The ratio of the weight loss due to the decomposition of carbonates (>600 °C in %) to that attributed to the loss of the structurally bound water to hydraulic products (200 °C - 600 °C in %), can provide important information about the hydraulic nature of the binder (Bakolas et al. 1998; Moropoulou et al. 2000, 2005). To Evaluate the type of mortar used in these monuments, it was used the index of hydraulicity of the mortar, defined as the ratio between the amount of CO₂ lost above 600 °C from carbonates and the amount of H₂O linked to hydraulic compounds, lost between 200 °C and 600 °C (Moropoulou et al. 1995, 2005). Consequently, higher CO₂/H₂O ratios correspond to less hydraulic mortars and lower CO₂/H₂O ratios to pozzolanic mortars.

	T<120 °C	120-200 °C	200-600 °C	600-800 °C	Total Loss	CO ₂ /H ₂ O
T-HR-1	2.20	1.23	5.46	12.32	21.22	2.26
T-HR-2	1.23	0.21	4.33	14.49	20.42	3.35
T-HR-3	1.53	0.52	2.53	12.15	16.71	4.80
T-HR-4	1.47	0.31	3.35	9.14	14.55	2.73
A-HR-1	1.27	0.64	3.76	11.89	17.91	3.16
A-HR-2	2.17	0.41	3.29	10.23	15.95	3.11
A-HR-3	1.28	0.71	3.52	5.75	11.26	1.63
A-HR-4	1.68	0.66	2.76	9.18	14.13	3.33
A-HR-6	2.32	0.41	3.28	11.79	17.73	3.59
A-HR-7	2.51	0.85	4.49	9.37	17.46	2.09
A-HR-8	0.26	0.10	1.07	4.15	5.37	3.88
A-HR-10	2.88	0.68	3.86	16.59	23.90	4.30
A-HR-11	1.37	0.39	2.05	10.89	14.65	5.31
A-HR-12	1.61	0.85	7.23	8.38	18.52	1.16

Table 3. CO₂/H₂O ratio in the mortar samples.

All the tested samples belong to hydraulic mortars, showing CO₂/H₂O ratio less than 10 and a relatively low amount of CO₂, less than 30% (Moropoulou et al., 2000). According to Moropoulou et al. (1995, 2005) and the results obtained for the mortars (Table 3), two types of mortars were found: samples T_HR-2, T_HR-3, A-HR-1, A_HR-2, A_HR-4, A_HR-6, A_HR-10, A_HR-11 and A_HR-12 could be

classified as artificial pozzolanic mortars due to their $\text{CO}_2/\text{H}_2\text{O}$ ratios were between 3 and 6, and the physically bound water (25 °C - 200 °C) and the structurally bound water (200 °C - 600 °C) according Moropoulou et al., (2005). In these samples were found aggregates in the form of ceramic fragments or ceramic powder (Fig. 6d). Samples T_HR-1, T-HR-4, A_HR-3 and A_HR-7, could be classified as lime mortars with unaltered portlandite due to the physically bound water (25 °C - 200 °C), the structurally bound water (200 °C - 600 °C) and the $\text{CO}_2/\text{H}_2\text{O}$ ratio. These mortars, which belong to structures many hundreds of years old, were extracted from areas having great thickness and where the carbonation process is slow under ordinary circumstances due to the percentage of carbon dioxide in the atmosphere is low. Samples A_HR-1 and T_HR-3 showed distinctive well marked endothermic peaks at 450°C and 850°C which indicate the dehydroxylation of portlandite ($\text{Ca}(\text{OH})_2$) and CSH, respectively. Samples T_HR-1, T_HR-4, A_HR-7 and A_HR-12 present endothermic peaks between 200°C-400°C.

6. Conclusions

Nowadays, there is the necessity to keep buildings and monuments that form part of the cultural World Heritage sites, through the realization of restoration and conservation interventions, some of them, with materials different to those originally used. These materials, in many cases, are not compatible with the original materials employed in their construction. We have to bear in mind that conservation interventions in historic buildings must be performed in a respectful way, without altering the distribution and appearance of the building. One way to achieve this objective is through the use of materials having petrological properties similar to the original ones.

The analysis of the concrete was carried out through petrographical and petrophysical analysis. The results obtained showed that the Roman concrete had lime as binder matrix completely carbonated and transformed to calcite. Three binder/aggregate ratios obtained were: 1:1; 1:2 and 1:3.

The medium-fine-grained, cohesive petrofabrics of the lime binders studied display a good aggregate bond, presence of pores, having different sizes, in the lime binder and some fissures. The aggregates mainly used are quartzite, schist, diorite, two-mica porphyritic granite and fragments of ceramic bricks. These aggregates come from waste materials from construction and from river sands near the city (Guadiana and Albarregas). Besides, it can be observed a greater presence of schist, having tremolite-actinolite in the aggregates, which come from the outcrop in the *arena* of the amphitheatre.

The compressive strength of the Roman concrete showed similar/slightly higher values to other ancient concretes, which could be due to the pozzolanic reaction. In the theatre, the shape of the aggregates, mainly rounded, and the pore size; large pores, having values around 1 mm, caused differences in the values of compression strength with samples belonging the amphitheatre, where angle-shaped aggregates lead to a better packed structure, decreasing large pores and increasing compression strength.

Through the thermogravimetric analysis and the index of hydraulicity of the mortar, two types of hydraulic mortars could be found, artificial pozzolanic mortar and lime mortars with unaltered portlandite.

There is a similarity in the mineralogical and petrological composition, aggregate rock fragments, of the theatre and the amphitheatre Roman concrete: the binder was composed by calcite (micrite); the aggregates showed heterogeneous composition (fragments of ceramic material, plant remains, fragments of granite rocks, quartzite, schist, diorite, porphyry, limestone and, quartz, feldspar and mica minerals) or aggregate sizes between fine, medium, coarse and gravel size. In regard to the aggregates of the Roman concretes from the amphitheatre, these showed larger sizes than those from theatre, besides in the amphitheatre, a greater use of rocks of schistose nature is observed due to the leveling geological of

substrate of zone SE. These, linked to the different binder/aggregate ratio in the Roman concrete between theatre (1:2) and the amphitheatre (1:3), could revealed us that both monuments were built on different ages, with different workers or less economics means.

Material weathering usually progresses over time however, in the samples studied, no relationship was found between the age of the mortar and its current condition, so these concretes were well preserved. It can be deduced from the petrographic analysis that the addition of ceramics fragments is partially responsible for the good quality and performance of these concretes.

Acknowledgments

Funding for this study was provided by the Autonomous Community of Madrid under the programmes: CLIMORTEC (National Project BIA2014-53911-R) from the Ministry of Economy and Competitiveness, GEOMATERIALES 2 (S2013/MIT-2914) and the Operational Programme for Cross-border Cooperation: Spain-Portugal (POCTEP-RITECA) 2007-2013. To the Consortium *Monumental Historical-Artistic and Archaeological City of Mérida* for providing us the legal authorization for sampling the monuments.

References

- Álvarez JI, Martín A, García Casado PJ, Navarro I, Zornoza A (1999) Methodology and validation of a hot hydrochloric acid attack for the characterization of ancient mortars. *Cem Concr Res* 29(7):1061-1066
- Arandigoyen M, Álvarez J (2006) Blended pastes of cement and lime: pore structure and capillary porosity. *Appl Surf Sci* 252:8077-85
- Arandigoyen M, Álvarez J (2007) Pore structure and mechanical properties of cement-lime mortars. *Cem Concr Res* 37:767-775
- Bakolas A, Biscontin G, Moropoulou A, Zendri E (1998) Characterization of Structural Byzantine Mortars by Thermogravimetric Analysis. *Thermochim Acta* 321:151-160
- Baronio G, Binda L (1986) Indagine sull'aderenza tra legante e laterizio in malte ed intonachi di 'cocciopesto'. *Bolletino d'Arte* 35-36:109-115
- Bendala Galán M, Durán Cabello R (1995) El anfiteatro de Augusta Emerita: rasgos arquitectónicos y problemática urbanística y cronológica, en el anfiteatro en la Hispania romana. *Coloquio Internacional, Mérida*, pp. 247–264 26-28 de Noviembre de 1992
- Borges C, Santos Silva A, Veiga R (2014) Durability of ancient lime mortars in humid environment. *Construct Build Mater* 66:606-620
- Cizer O, Van Balen K, Van Gemert D, Elsen J (2008) Blended lime–cement mortars for conservation purposes: microstructure and strength development. In: *Structural analysis of historic construction: preserving safety and significance – proceedings of the 6th international conference on structural analysis of historic construction, SAHC08 2, United Kingdom*, 965-972
- Collepari M (1990) Degradation and restoration of masonry walls of historical buildings. *Mater Struct* 23(2):81-102
- Chen X, Wu S, Zhou J (2013) Influence of porosity on compressive and tensile strength of cement mortar. *Constr Build Mater* 40:869-874
- D'Ambrosio E, Marra F, Cavallo A, Gaeta M, Ventura G (2015) Provenance materials for Vitruvius' harenae fossiciae and pulvis puteolanis: geochemical signature and historical-archaeological implications. *J Archaeol Sci Rep* 2:186-203
- Drdácky M, Fratini F, Frankeova D, Slizkova Z (2013) The Roman mortars used in the construction of the Ponte di Augusto (Narni, Italy). A comprehensive assessment. *Constr Build Mater* 38:1117-1128
- Durán Cabello RM (2004) El teatro y el anfiteatro de Augusta Emerita. *Contribución al conocimiento histórico de la capital de Lusitania*. Archaeopress, Oxford *BAR International Series*; 1207
- Elpida-Chrissy A, Eleni-Eva T, Elizabeth V (2008) Lime–pozzolan-cement compositions for the repair and strengthening of historic structures. In: *International conference HMC 08 – historical mortars conference: characterization, diagnosis, repair and compatibility*. Lisbon, Portugal: LNEC
- Elsen J (2006) Microscopy of historic mortars-a review. *Cem Concr Res* 36:1416-1424

- Farci A, Floris D, Meloni, P (2005) Water permeability vs. porosity in samples of Roman mortars. *J Cult Heritage* 6:55-59
- Flatt RJ (2002) Salt damage in porous materials: how high supersaturations are generated. *J Crys Growth* 242:435-454
- Fernández-Caliani JC, Galán E, Liso MJ (1996) Mineralogía, geoquímica y evolución diagenética de los materiales carbonatados del área de Mérida (Badajoz). *Estudios Geol* 52:3-9
- Fort R, Álvarez de Buergo M, Pérez-Montserrat E, Varas MJ (2010) Characterisation of monzogranitic batholiths as a supply source for heritage construction in the northwest of Madrid. *Eng Geol* 115:149-157
- Franquelo ML, Robador MD, Ramírez-Valle V, Duran A, Jiménez de Haro MC, Pérez-Rodríguez JL (2008) Roman ceramics of hydraulic mortars used to build the Mithraeum House of Mérida, Spain. *J Therm Anal Cal* 92:331-335
- Genestar C, Pons C, Más A (2006) Analytical characterisation of ancient mortars from the archaeological Roman city of Pollentia (Balearic Islands, Spain). *Anal Chem Acta* 557:373-379
- Giavarini C, Ferretti AS, Santarelli ML (2006) Mechanical characteristics of Roman “opus caementicium”. In: Kourkoulis SK. (ed.) *Fracture and Failure of Natural Building Stones*, Springer, Berlin, pp 107-120
- Gleize PJP, Motta EV, Silva EV (2009) Roman HR. Characterization of historical mortars from Santa Catarina (Brazil). *Cem Concr Com* 31(5):342-346
- Gonzalo JC (1987). *Petrología y estructura del basamento en el área de Mérida (Extremadura Central)*. Doctoral Thesis. Universidad de Salamanca.
- Hughes D, Swann S, Gardner A (2007) Roman cement: part one, its origins and properties. *J Archit Conserv* 13:21-36
- Kramar S, Zala V, Urosevic M, Körner W, Mauko A, Mirtiç B, Lux J, Mladenovic A (2011) Mineralogical and microstructural studies of mortar from the bath complex of the Roman Villa rustica near Mošnje (Slovenia). *Mat Charac* 62:1042-1057
- Laskar AI, Kumar R, Bhattacharjee B (1997) Some aspects of evaluation of concrete through mercury intrusion porosimetry. *Cem Concr Res* 27(1):93-105
- Liñán E and Perejón A (1981) El Cámbrico inferior de la Unidad de Alconera, Badajoz (SO España). *Bol. R. Soc Esp Hist Nat (Sec. Geol.)* 79:125-148
- Lourenço P (2006) Recommendations for restoration of ancient buildings and the survival of a masonry chimney. *Construct Build Mater* 20:239-251
- MAGNA 2003. *Mapa Geológico de España 1:50.000. Mérida (777)*. Instituto Tecnológico Geominero de España. 69 pp
- Malacrino CG (2010) *Constructing the ancient world. Architectural techniques of the Greeks and Romans*

- Malinowski R (1979) Concrete and mortar in ancient aqueducts. *Concr Int* 1:66-76
- Malinowsky R (1991) Prehistory of concrete. *Concr Int*; 13:62-8
- Marra F, Danti A, Gaeta M (2015) The volcanic aggregate of ancient Roman mortars from the Capitoline Hill: Petrographic criteria for identification of Rome's "pozzolans" and historical implications. *J Volc Geo Res* 308:113-126
- Mateos P (2001) Augusta Emerita. La investigación arqueológica en una ciudad de época romana. *AespA* 74:183–208
- Mateos P, Pizzo A (2011) Los edificios de ocio y representación. El teatro y el anfiteatro de Augusta Emerita. In: *Actas Congreso Internacional 1910–2010: El Yacimiento Emeritense*, 173–194
- Moropoulou A, Bakolas A, Bisbikou K (1995). Characterization of ancient, byzantine and later historic mortars by thermal analysis and X-ray diffraction techniques. *Thermochim Acta* 269:779-795
- Moropoulou A, Cakmak AS, Biscontin G (1998a) Criteria and methodology to evaluate the Hagia Sophia crushed brick/lime mortars. *Journal of the European Study Group on Physical, Chemical, Biological and Mathematical Techniques Applied to Archaeology* 55:39-54
- Moropoulou A, Maravelaki-Kalaitzaki P, Borboudakis M, Bakolas A, Michailidis P, Chronopoulos M (1998b) Historic mortars technologies in Crete and guidelines for compatible restoration mortars. *Journal of the European Study Group on Physical, Chemical, Biological and Mathematical Techniques Applied to Archaeology* 55:55-72
- Moropoulou A, Bakolas A, Bisbikou K (2000) Investigation of the technology of historic mortar. *J Cult Herit* 1(1):45-58
- Moropoulou A, Cakmak AS, Biscontin G, Bakolas A, Zendri E (2003) Advanced Byzantine cement based composites resisting earthquake stresses: the crushed brick/lime mortars of Justinian's Hagia Sophia. *Construct Build Mater* 16:543-552
- Moropoulou A, Bakolas A, Anagnostopoulou S (2005) Composite materials in ancient structures. *Cem Concr Com* 27:295-300
- Mosquera M, Benitez D, Perry S. (2002) Pore structure in mortars applied on restoration: effect on properties relevant to decay of granite buildings. *Cem Concr Res* 32:1883-1891
- Ortiz P, Antúnez V, Martín JM, Ortiz R, Vázquez MA, Galán E (2014) Approach to environmental risk analysis for the main monuments in a historical city. *J Cult Herit* 15(4):432-440
- Paama L, Pitkanen I, Ronkkomaki H, Peramaki P (1998) Thermal and infrared spectroscopic characterization of historical mortars. *Thermochim Acta* 320(1–2):27-33
- Pacheco-Torgal F, Faria J, Jalali S (2012) Some considerations about the use of lime–cement mortars for building conservation purposes in Portugal: A reprehensible option or a lesser evil?. *Construct Build Mater* 30:488-494

Pavía S, Bolton J (2000) Stone, brick of mortar: historical, use decay and conservation of building material in Ireland. Ed Wordwell Ltd

Pavía S, Caro S (2008) An investigation of Roman mortar technology through the petrographic analysis of archaeological material. *Constr Build Mater* 22:1807-1811

Pizzo A (2007) Las técnicas constructivas de la arquitectura pública de Augusta Emérita. PhD Thesis, Universidad Autónoma de Madrid, October, 2007

Robador MD, Pérez-Rodríguez JL, Durán A (2010) Hydraulic structures of the Roman Mithraeum house in Augusta Emerita , Spain. *J Arch Sci* 37:2426-2432

Roy DM, Langton C (1989) Studies of ancient concretes as analogs of cementitious sealing materials for repository in Tuff. L A- 11527-MS. Los Alamos National Laboratory

Sánchez-Moral S, García-Guinea J, Luque L, González-Martín R, López-Arce P (2004). Carbonation cinetics in roman-like lime mortars. *Mater Constr* 54:23-37

Sandrolini F, Franzoni E (2010) Characterization procedure for ancient mortars' restoration: The plasters of the Cavallerizza courtyard in the Ducal Palace in Mantua (Italy). *Mat Charac* 61:97-104

Scherer GW (1999) Crystallization in pores. *Cem Concr Res* 29(8):1347-1358

Theodoridou M, Ioannou I, Philokyrou M (2013) New evidence of early use of artificial pozzolanic material in mortars. *J Arch Sci* 40:3263-3269

Tucci PL (2014) The Oxford handbook of Greek and Roman art and Architecture. The Materials and Techniques of Greek and Roman Architecture. Clemente Marconi ed

UNESCO: <http://whc.unesco.org/es/list/664>

Varas MJ, Álvarez de Buergo M, Fort R (2005) Natural cement as the precursor of Portland cement: Methodology for its identification. *Cem Concr Res* 35:2055-2065

Velosa AL, Coroa J, Veiga MR, Rocha F (2007) Characterisation of roman mortars from Conímbriga with respect to their repair. *Mat Charac* 58:1208-1216

Winkler EM (1997) Stone in Architecture: Properties, Durability. 3rd ed. Springer-Verlag, Berlin

Zamba IC, Stamatakis MG, Cooper FA, Themelis PG, Zambas CG (2007) Characterization of mortars used for the construction of Saithidai Heroon Podium (1st century AD) in ancient Messene, Peloponnesus, Greece. *Mat Charac* 58:1229-1239